

Contrast-dependence of surround suppression in Macaque V1: Experimental testing of a recurrent network model

Lars Schwabe^{a,1}, Jennifer M. Ichida^{b,1}, S. Shushruth^b, Pradeep Mangapathy^b, Alessandra Angelucci^{b,*}

^a Adaptive and Regenerative Software Systems, Department of Computer Science and Electrical Engineering, University of Rostock, Albert-Einstein-Str. 21, 18059 Rostock, Germany

^b Department of Ophthalmology and Visual Science, Moran Eye Center, University of Utah, 65 Mario Capecchi Drive, Salt Lake City, UT 84132, USA

ARTICLE INFO

Article history:

Received 25 September 2009

Revised 3 December 2009

Accepted 11 January 2010

Available online 15 January 2010

ABSTRACT

Neuronal responses in primary visual cortex (V1) to optimally oriented high-contrast stimuli in the receptive field (RF) center are suppressed by stimuli in the RF surround, but can be facilitated when the RF center is stimulated at low contrast. The neural circuits and mechanisms for surround modulation are still unknown. We previously proposed that topdown feedback connections mediate suppression from the “far” surround, while “near” surround suppression is mediated primarily by horizontal connections. We implemented this idea in a recurrent network model of V1. A model assumption needed to account for the contrast-dependent sign of surround modulation is a response asymmetry between excitation and inhibition; accordingly, inhibition, but not excitation, is silent for weak visual inputs to the RF center, and surround stimulation can evoke facilitation. A prediction stemming from this same assumption is that surround suppression is weaker for low than for high contrast stimuli in the RF center. Previous studies are inconsistent with this prediction. Using single unit recordings in macaque V1, we confirm this model's prediction. Model simulations demonstrate that our results can be reconciled with those from previous studies. We also performed a systematic comparison of the experimentally measured surround suppression strength with predictions of the model operated in different parameter regimes. We find that the original model, with strong horizontal and no feedback excitation of local inhibitory neurons, can only partially account quantitatively for the experimentally measured suppression. Strong direct feedback excitation of V1 inhibitory neurons is necessary to account for the experimentally measured surround suppression strength.

© 2010 Elsevier Inc. All rights reserved.

Introduction

A major goal of vision research is to understand how neural circuits compute the responses of cortical neurons. In the primary visual cortex (V1), responses of neurons to optimally oriented, high contrast stimuli inside the receptive field (RF) are suppressed by iso-oriented stimuli in the RF surround (Allman et al., 1985; Blakemore and Tobin, 1972; DeAngelis et al., 1994; Gilbert and Wiesel, 1990; Nelson and Frost, 1978). Surround suppression may represent the neural substrate for perceptual figure-ground and/or texture segmentation (Knierim and van Essen, 1992; Lamme, 1995; Li, 1999; Malik and Perona, 1990), or for detection of salient targets for subsequent saccades (Petrov and McKee, 2006); alternatively, it may reflect optimal coding of visual information (Rao and Ballard, 1999; Schwartz and Simoncelli, 2001), or statistical inference operations in the visual cortex (Friston, 2005; Harrison et al., 2007). The neural circuits and mechanisms for surround suppression remain unknown. Statistical models have been proposed that accurately describe the

interactions between the RF and surround of V1 neurons (e.g. the difference, or ratio, of Gaussian models; Cavanaugh et al., 2002a; Sceniak et al., 1999, 2001). However, these models, by virtue of their design, can only hint at underlying mechanisms, and while they can inter- and extrapolate from measured data, they do not offer the predictions one can derive from mechanistic neuronal network models. We have developed a network model for surround suppression in V1, which incorporates feedback connections from extrastriate cortex, and can account for many experimental findings using only one set of parameters (Schwabe et al., 2006). Feedback connections are generally believed to serve attentional (Maunsell and Treue, 2006) and other task-related top-down modulations (Navalpakkam and Itti, 2007; Salinas, 2006; Schwabe and Obermayer, 2005), or to play a role in perceptual learning (Li et al., 2008; Schäfer et al., 2007). However, we (Angelucci and Bressloff, 2006) have recently proposed that these connections, which have a much larger spatial scale (Angelucci et al., 2002) and are much faster-conducting (Girard et al., 2001) than intra-V1 horizontal connections, may also generate surround modulation in V1 (Fig. 1a). In our model, feedback mediates the modulatory effects of the “far” surround, which we define as the visual field region beyond the spatial extent of V1 horizontal connections, while “near” surround modulation is mediated by both feedback and horizontal

* Corresponding author. Fax: +1 801 587 7820.

E-mail address: alessandra.angelucci@hsc.utah.edu (A. Angelucci).

¹ These authors contributed equally to this work.

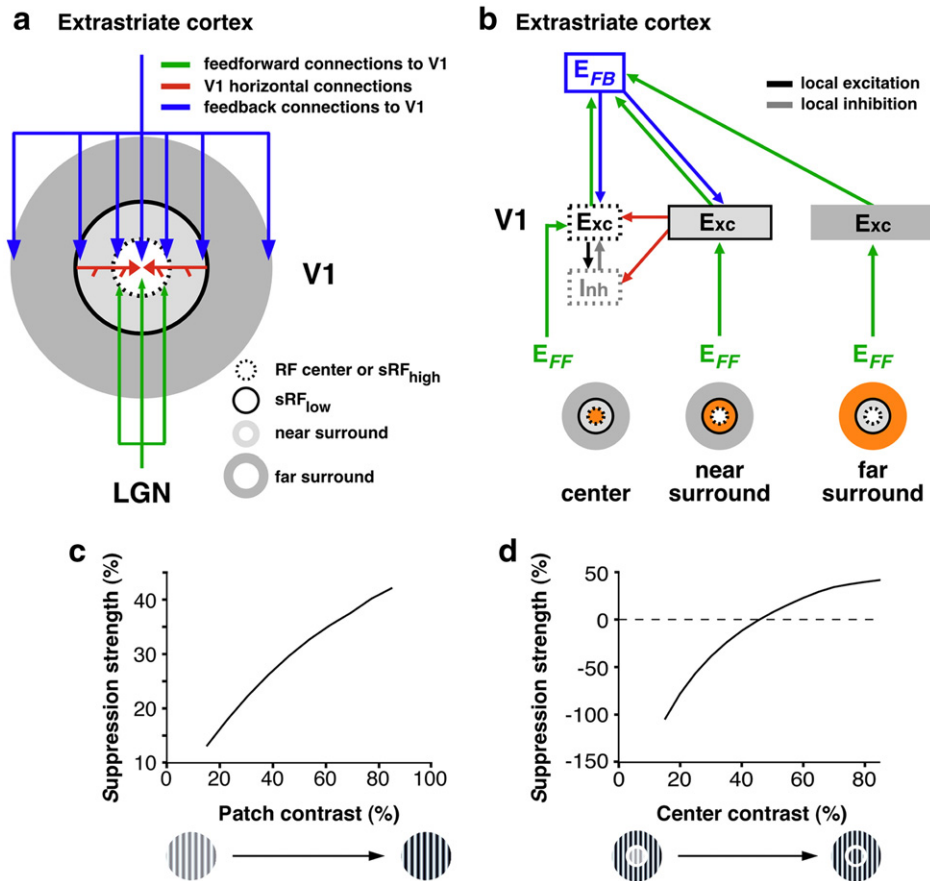


Fig. 1. Presumptive anatomical substrates for the RF center and surround of V1 neurons, and the recurrent network model. (a) Diagram of the different components of the RF center and surround of a typical V1 neuron: (i) the high-contrast summation RF (sRF_{high}; white area inside dashed circle), and (ii) the low-contrast summation RF (sRF_{low}; area inside solid black circle) are measured by presenting high- or low-contrast grating patches, respectively, of increasing radius, and defined as the grating's radius evoking the largest response from the V1 cell (e.g. see left panels in Fig. 2); (iii) the "near" surround (light gray annulus) is the region between the sRF_{high} and sRF_{low}; (iv) the far surround (dark gray annulus) is the region outside the sRF_{low}. Feedforward connections (green) to V1 from the lateral geniculate nucleus (LGN) are commensurate with the sRF_{high} of V1 neurons (Angelucci and Sainsbury, 2006). Intra-areal V1 horizontal connections (red) are commensurate with the sRF_{low}, while extrastriate feedback connections (blue) to V1 are commensurate with the full spatial scale of the center and surround field of V1 neurons (Angelucci et al., 2002). (b) Diagram of the architecture of the recurrent network model of center-surround interactions proposed by Schwabe et al. (2006). Only the major afferent pathways that more directly affect the response of the center excitatory and inhibitory neurons are shown. For the full network architecture see Schwabe et al. (2006). Different connection types are indicated as color-coded arrows (according to legends in panels a and b). Dashed boxes: populations of excitatory (Exc) or inhibitory (Inh) V1 neurons in the RF center; filled gray boxes: population of excitatory neurons with RF centers positioned in the near and far surround. E_{FF}: excitatory neurons in other V1 layers sending feedforward afferents to Exc neurons in V1 layers 2/3. E_{FB}: excitatory neurons in extrastriate cortex sending feedback projections (blue arrows) to Exc neurons in V1. Note that here for simplicity we only depicted feedback neurons in the extrastriate cortex whose RF centers overlap the RF center of V1 neurons. However, in the full model feedback neurons also lie in the near and far surround; importantly irrespective of their RF center location, any of these feedback neurons can affect the response of V1 neurons in the center, near and far surround, because of the high anatomical divergence of their axons. Icons at the bottom: different components of the RF center and surround (as in panel a), with orange areas indicating the components that are activated when each respective network module is active. (c)–(d) Contrast-dependence of surround suppression strength predicted by the recurrent network model. Model simulation of the strength of surround suppression as a function of stimulus contrast. In (c), the stimulus consisted of a large grating patch covering the RF center as well as the near and far surround, and suppression strength was measured as indicated in Fig. 3a. Note that suppression strength increases with stimulus contrast. In (d), the stimulus consisted of a center grating fitted to the size of the cell's sRF_{high}, whose contrast was systematically varied; this was surrounded by an annular grating confined to the far surround of fixed high contrast (75%). Suppression strength was measured as indicated in Fig. 4a. Positive values of suppression strength indicate response suppression, while negative values indicate response facilitation. Note that suppression strength increases with increasing contrast of the grating in the RF center.

connections (Schwabe et al., 2006) (Figs. 1a, b). Similar to a previous model (Dragoi and Sur, 2000; Somers et al., 1998), our model accounts for suppression via intra-cortical inhibition.

Two important features characterize our model. First, the assumption of feedback targeting exclusively excitatory, but not inhibitory neurons (Fig. 1b), a constraint that was imposed by experimental findings in rat visual cortex (Johnson and Burkhalter, 1996; Shao and Burkhalter, 1996); these were the only anatomical data available at the time we generated our model (see Discussion). Thus, in the model far surround suppression is generated by feedback connections targeting excitatory neurons in the near surround, which in turn send horizontal connections to local inhibitory neurons in the RF center (Fig. 1b). Second, the assumption of a higher functional threshold and response gain of inhibitory neurons, compared to excitatory neurons; this feature is needed to account for the contrast-

dependence of surround modulation. Specifically, because of this response asymmetry between excitation and inhibition in the model, the high-threshold inhibitory neurons are silent for weak visual inputs presented to the RF center (e.g. low contrast stimuli), and stimulation of the near or far surround generates facilitation. Near surround facilitation at low center stimulus contrast has been observed experimentally (Polat et al., 1998; Sceniak et al., 1999). Recently, we have also confirmed experimentally the model's prediction of far surround facilitation at low center stimulus contrast (Ichida et al., 2007). An additional prediction of the model, stemming from the same assumption of response asymmetry between excitation and inhibition, is the dependence of the strength of surround suppression on the contrast of the stimulus presented to the RF center. Specifically, at low center stimulus contrast, the strength of near or far surround suppression is predicted to be weaker than at high contrast

(Figs. 1c, d). Published data on the relationship between contrast and surround suppression strength are contradictory and inconsistent with our model's prediction, showing either no relationship between contrast and suppression strength (Sceniak et al., 1999), or stronger suppression for center stimuli of lower contrast (Cavanaugh et al., 2002a; Levitt and Lund, 1997; Sadakane et al., 2006). Therefore, we have re-examined this issue experimentally. Our electrophysiological results are consistent with the model's prediction of weaker suppression at low stimulus contrast, and can be reconciled with apparently contradictory results from previous studies.

A second goal of this study was to investigate how well the model can account quantitatively for the suppression strength seen in the data. To this purpose, we systematically compared our data with the predictions of our model operated in different parameter regimes. We find that the original published model (Schwabe et al., 2006) can account quantitatively for the far surround data, but cannot fully account for the near surround data. The parameter regime that best describes the data quantitatively includes stronger feedback excitation of local inhibition than we assumed in the original model. However, additional suppression needed in the model to account for near surround data could also arise from surround suppression of geniculate afferents, which is missing in the current version of our model.

Materials and methods

Surgical preparation and recording

We recorded extracellularly in V1 of five anesthetized (sufentanil citrate, 4–12 $\mu\text{g}/\text{kg}/\text{h}$) and paralyzed (vecuronium bromide, 0.1 $\mu\text{g}/\text{kg}/\text{h}$) macaque monkeys (*Macaca fascicularis*). Animals were respiration with a 30:70 mixture of O_2 and N_2O . The electrocardiogram was continuously monitored, end tidal CO_2 was maintained between 30 and 33 mm Hg, rectal temperature near 37 °C and blood oxygenation near 100%. The pupils were dilated with tropical atropine and the corneas protected with rigid gas-permeable contact lenses. The locations of the foveas were plotted at the beginning of the experiment and periodically thereafter. Supplementary lenses were used to focus the eyes on the display screen.

Single unit recordings were made with tungsten microelectrodes (4–6 M Ω ; FHC, Bowdoin, ME) in the opercular region of V1. Spikes were amplified, filtered, and sampled at 22 kHz by a dual processor G5 Power Macintosh computer running the custom software EXPO, kindly donated to us by Dr. Peter Lennie. Spikes were displayed on a monitor, and templates for discriminating spikes were constructed by averaging multiple traces. The timing of waveforms that matched the templates was recorded with an accuracy of 0.1 ms. All procedures conformed to the guidelines of the University of Utah Institutional Animal Care and Use Committee.

Visual stimuli and characterization of receptive fields and surround fields

Sinusoidal gratings of the same mean luminance as the background were generated by the same software and computer that recorded spikes, and were displayed on a calibrated monitor (Sony GDM-C520K) refreshed at 100 Hz of mean luminance $\sim 45.7 \text{ cd}/\text{m}^2$, at a viewing distance of 57 cm (at which the screen subtended a visual angle of 28°). For each cell, we first determined the preferred orientation, spatial and temporal frequency. Then, the diameter and geometric center of the minimum response field (mRF) were carefully located quantitatively using a grating patch of 0.1° radius. Using a grating patch matched to the cell's mRF diameter, we generated a contrast response function for each cell and used the individual cell responses to tailor the contrast values for the remaining stimuli. High contrast values were chosen so that neuronal responses did not exceed 90% of response saturation for the cell (typically between 50%

and 80% contrast); low contrast values were generally chosen to be those eliciting <50% of the maximum response in the cell's contrast-response function, but still eliciting a reliable response (at least 2 SD greater than the spontaneous firing rate; typically between 4% and 30%; the cell in Fig. 2c was one exception).

RF and surround size measured by the expanding patch method

We performed spatial summation measurements at high and low contrast, using circular patches of drifting gratings of increasing radius centered over the cell's mRF. The patch radius ranged from 0.1° to 14° and consisted of 11 radii presented in random order within each block of trials (0.1°, 0.2°, 0.4°, 0.8°, 1.2°, 1.6°, 2.5°, 5°, 7.5°, 10°, 14°). From these patch-size tuning curves at high and low contrast we extracted for each cell the patch radius at peak response. The radii at peak response in the low- and high-contrast conditions are referred to as the summation receptive fields at low (sRF_{low}) and high (sRF_{high}) contrast (see Fig. 1a). The latter were used to create the center and annular surround stimuli used for the “expanding annulus method” described in the text below.

Surround size measured by the expanding annulus method

In this experimental protocol, the RF center was stimulated with a grating patch of optimal stimulus parameter for the recorded cell fitted to the radius of the cell's sRF_{high}; this was surrounded by an annular grating with a fixed outer radius (14°) and an inner radius whose size was systematically decreased from 12.5° to a size \geq the sRF_{low} of the cell (we used nine annulus inner radii). Thus, there was always a blank annulus of the same luminance as the background interposed between the center grating patch and the surround annular grating, i.e. covering the near surround. For this stimulus, we used the same two contrast values, high and low, as used for the expanding patch method, with the contrast of the center and surround gratings being controlled independently. We used three different combinations of center and annulus contrast: high center and high annulus contrast (HH), low center and high annulus contrast (LH), and low center and low annulus contrast (LL). The center and surround gratings had otherwise identical stimulus parameters (orientation, drift direction, spatial phase, spatial and temporal frequency).

Control conditions included a blank screen (of the same luminance as the background) for a measure of spontaneous activity, a center-alone condition for a baseline response, and a surround annulus-alone condition to ensure that the surround stimulus alone did not drive a response. For the latter measurement we used the surround annulus with smallest inner radius (i.e. the widest surround annulus) that was used to measure surround suppression in the center-plus-surround condition.

Both annular and patch stimuli were presented randomly in a block-wise fashion with a duration of 2 s and a 2 s inter-stimulus interval. Each block was repeated 10 times and the responses across blocks were averaged to calculate the mean firing rate for each stimulus condition.

Data analysis

Statistical model fitting

Both the patch-size and annulus-size tuning data were fit with a “thresholded” difference of Gaussian (t-DOG) model, as previously described (Ichida et al., 2007). This is because, the t-DOG model, unlike the more standard difference (or ratio) of Gaussian model (DOG or ROG, respectively), captures well the far surround facilitation. Briefly, the t-DOG model describes excitation and inhibition as two Gaussian functions of identical spatial scales, with the inhibition becoming effective after a threshold is crossed.

In order to compare our measure of surround suppression with the DOG-model-based quantification of surround suppression performed

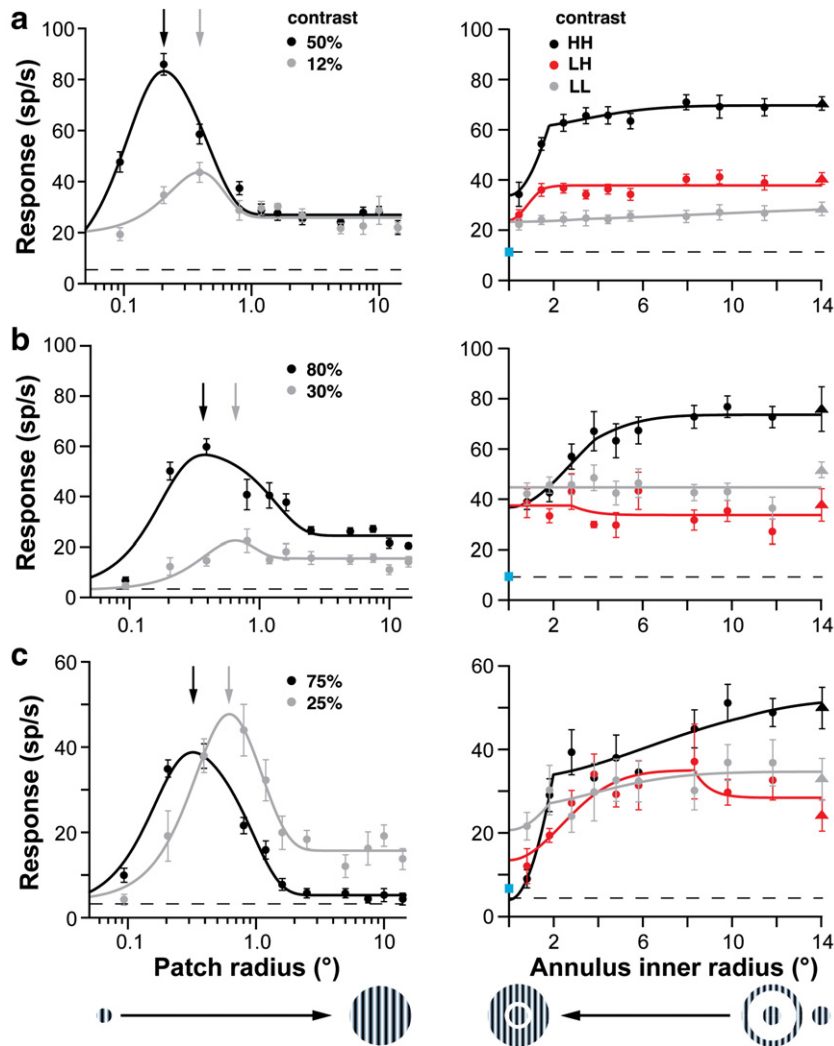


Fig. 2. Patch-size and annulus size tuning curves for three example V1 cells showing weaker surround suppression at low contrast. (a–c, left) Responses (mean firing rate) of 3 V1 cells as a function of the radius of a circular optimal grating patch (stimulus shown in c). *Black and gray curves*: responses to a high or low contrast grating patch, respectively; contrast values used are indicated in each panel. *Solid lines* represent fits to the data (*dots*) using the DOG model (see [Materials and methods](#)). *Dashed lines*: cell's mean spontaneous firing rate. *Arrows*: radius of the high (*black*) or low (*gray*) contrast stimulus evoking the largest response from the cell, i.e. the sRF_{high} and sRF_{low} , respectively. Error bars are s.e.m. The suppression strength (SS_{patch} , see [Materials and methods](#)) at high and low contrast for each cell was: 74.4% and 49.7% (a), 65% and 36% (b), 88% and 69% (c). (a–c, right) Responses of the same three cells as a function of the inner radius of an annular grating in the far surround (stimulus shown in c). *Black, red and gray curves*: responses in the HH, LH and LL contrast conditions, respectively. High and low contrasts used are the same as indicated in each respective left-hand panel. *Triangles (rightmost data point)*: responses to center-only stimulation. *Blue squares*: responses to the largest surround-only stimulus. *Solid lines*: fits to the data using the t-DOG model. The suppression strength ($SS_{annulus}$, see [Materials and methods](#)) in the HH, LH and LL condition for each cell was: 48%, 31% and 17% (a); 47%, -11% and 5% (b); 53%, 37% and 25% (c).

in a previous study (Sceniak et al., 1999), we also fit the patch-size tuning data with the difference of the integral of two Gaussian functions (DOG model), as in Sceniak et al. (1999, 2001), and as we did previously (Shushruth et al., 2009). Specifically, each patch-size tuning curve was least-square fit using the function

$$R(s) = R_0 + K_e \int_{-s/2}^{s/2} \exp(-[2y/a]^2) dy - K_i \int_{-s/2}^{s/2} \exp(-[2y/b]^2) dy$$

with R_0 , K_e , K_i , a and b being free model parameters. Here, the values of a and b determine the spatial scale of the excitatory and inhibitory Gaussians, respectively.

The values of the free parameters in both models were optimized to produce the best least-squares fit to the data. The analysis for the patch-size tuning data was performed on both the fitted and raw data; both yielded similar results, but in [Results](#) section we report only the analysis based on the raw data. The analysis for the annulus-size tuning data reported in [Results](#) instead was based on the t-DOG fits.

Measures of surround suppression strength

From the patch-size tuning data we calculated the strength of surround suppression as:

$$SS_{patch} = 100 \times \frac{R_{max} - R_{largest_patch}}{R_{max}}$$

where R_{max} is the maximal response (over all patch sizes), and $R_{largest_patch}$ is the response to the largest patch size.

To compare our data with those of Sceniak et al. (1999), in [Fig. 3b](#), after fitting patch-size tuning curves with the DOG model function, we calculated surround suppression strength as

$$SI = \frac{K_i b}{K_e a}$$

This measure is the ratio of the area under the inhibitory Gaussian over that of the excitatory Gaussian.

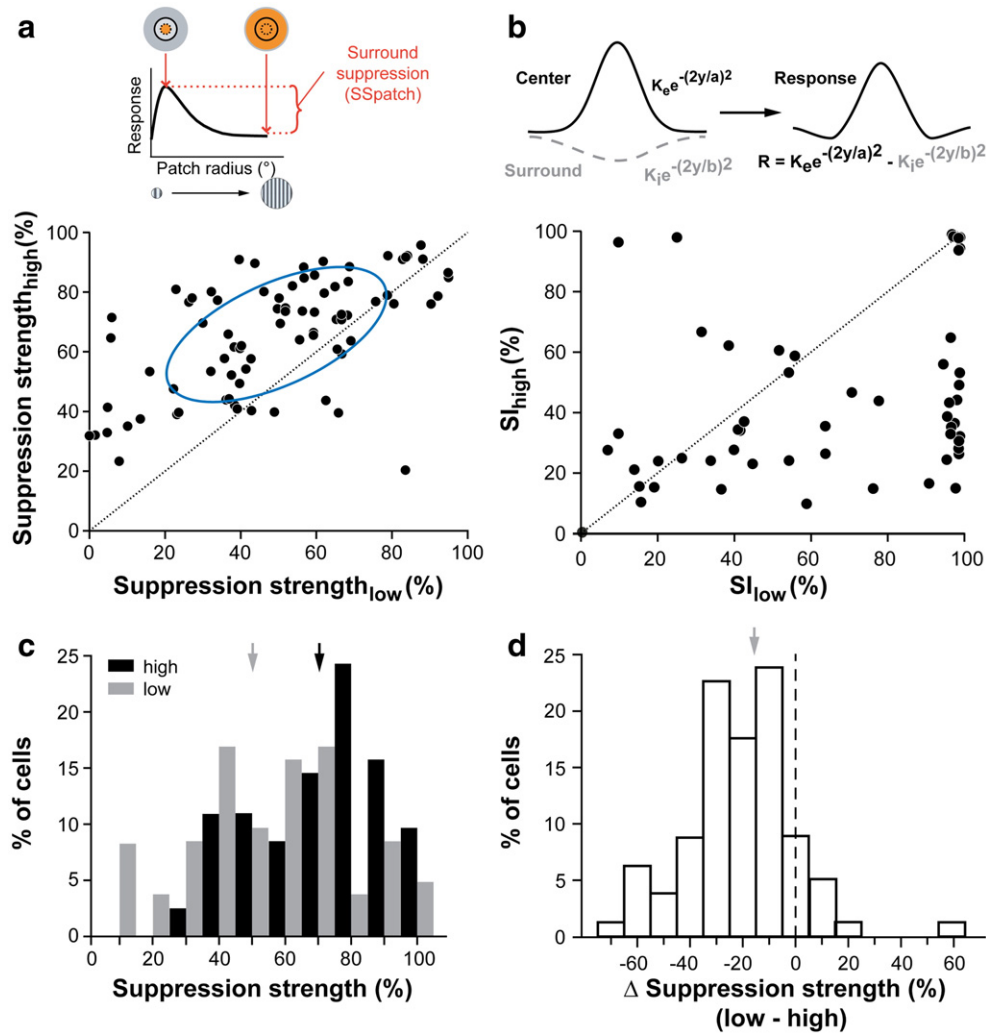


Fig. 3. Contrast-dependence of surround suppression strength measured with the expanding patch protocol. (a) *Top inset:* method used to compute the strength of suppression from patch-size tuning curves (see also [Materials and methods](#)). *Bottom:* Scatter plot of surround suppression strength (SS_{patch}) at high vs. low contrast, quantified using the method indicated in the inset. The *blue ellipse* indicates the 50% confidence interval of a Gaussian fit to the measured data, with its center representing the mean suppression strength ($65.8\% \pm 2.1$ and $49\% \pm 2.8$ for high and low contrast, respectively; $n = 80$ cells). (b) Scatter plot of suppression strength at high vs. low contrast, quantified from the DOG model's fits (indicated in the *inset at the top of b*) to the patch-size tuning data, as the ratio of the area under the inhibitory Gaussian over the area under the excitatory Gaussian (as in [Sceniak et al., 1999](#)). (c) Distribution of suppression strength at high (*black*) and low (*gray*) stimulus contrast, measured as described in (a). Larger values indicate stronger response suppression. *Arrows:* medians (*black* = 70.8%; *gray* = 50.3%). (d) Distribution of the change (Δ) in suppression strength with contrast (measured as: SS_{patch} at low contrast - SS_{patch} at high contrast), computed for each cell. Negative (positive) values of Δ indicate that suppression was weaker (stronger) at low contrast. *Arrow:* median (-15.9%).

The strength of far surround suppression was instead measured from the annulus-size tuning data fit with the t-DOG model, as:

$$SS_{\text{annulus}} = 100 \times \frac{R_{\text{ctr}} - R_{\text{inner}}}{R_{\text{ctr}}},$$

where R_{ctr} is the response to the center stimulus alone, and R_{inner} is the response to the center stimulus plus the annular surround grating. As the inner radius of this annulus we took

$$R_{\text{inner}} = \max(4 \times \text{sRF}_{\text{high}}, \text{sRF}_{\text{low}})$$

This is because the sRF_{low} is approximately two times larger than the sRF_{high} ([Sceniak et al., 1999](#); [Shushruth et al., 2009](#)), and it is on average coextensive with the length of V1 horizontal connections ([Angelucci et al., 2002](#)). Thus, using as a conservative measure of near surround ($4 \times \text{sRF}_{\text{high}}$), we ensured that the annular surround grating was always beyond the approximate extent of horizontal connections, i.e. in the far surround.

The recurrent network model

We used the network model from [Schwabe et al. \(2006\)](#) with *exactly the same parameterization*. The only parameters varied were the strengths of horizontal and feedback connections to inhibitory neurons; this was done in order to explore the effects of these model parameters on suppression strength, and to compare predicted suppression strength with experimentally measured suppression strength. The complete model description is given in [Schwabe et al. \(2006\)](#); the model description, including all parameter values, is also reported in the [Supplementary Material](#). A simplified diagram of the model's architecture is illustrated in [Fig. 1b](#). Note, however, that the actual network model was a recurrent model with two layers (V1 and area MT) being modeled as one-dimensional arrangements of pairs of excitatory and inhibitory model neurons, with the excitatory neurons making inter-areal feedback and intra-areal horizontal connections. The weights of these connections depend on the distance between the pre- and post-synaptic neurons' RF centers. Specifically, neurons with overlapping RF centers in V1 and the extrastriate area have strongest

inter-areal connections; as the distance between RF centers increases, the connection strength decreases exponentially with a space constant determined by our anatomical data (see [Supplementary Material](#) for relative equations). Here, the important feature of these connections is that the space constant for horizontal connections is much smaller than for inter-areal feedback connections (Fig. 1a).

Comparison of model predictions with experimental data

Since the network model is a mean-field model, which does not account for the variability among cells we found in the data, we had to derive a simple way of comparing the model predictions with the data. We assume that the variability in the measured data is the result of different cells having their own different circuits (e.g. with different weights of horizontal, feedforward, and feedback connectivity), possibly corresponding to the set of circuits we are exploring in terms of different model parameterizations. Instead of deriving *ad hoc* “noise models” for our recurrent mean-field network, to account for the variability in the data, we adopted the following procedure. First, we determined the parameters of a Gaussian fit to the suppression data, i.e. the mean suppression and the covariance matrix for all conditions in the patch-size and annulus-size tuning data. This gave rise to a five-dimensional multivariate Gaussian probability distribution. Then, we determined the probability of the predicted suppression strengths, given this probabilistic description of our data. This allows for a simple comparison of different model parameterizations in terms of how compatible they are with the measured data. In other words, we asked “How likely is it that we observe the predicted responses” as opposed to “How likely are the observed responses given our model predictions”.

Results

The goal of this study was to test a specific model prediction on the contrast-dependence of surround suppression, namely that near and far surround suppression are weaker when the RF center is stimulated at low contrast (Figs. 1c, d). The second goal of this study was to compare quantitatively the strength of surround suppression measured in the data with the suppression strength predicted by the model operated in different parameter regimes. These results are presented in two parts. In the first part, we present electrophysiological data on the contrast-dependence of surround suppression. In the second part, we present a data-model comparison.

To measure the strength of *near* surround suppression we used the expanding patch method described in [Materials and methods](#). In effect this stimulus (shown in the left panel of Fig. 2c) activates all surround regions, i.e. both near and far, in addition to the RF center; however, we ([Ichida et al., 2007](#)) and others ([Levitt and Lund, 2002](#)) have previously shown that it reveals predominantly the stronger modulatory effects of near surround stimulation. To measure the strength of *far* surround suppression, instead, we used the expanding annulus method (see [Materials and methods](#); stimulus shown on the right panel of Fig. 2c). By masking out the near surround, this stimulus allowed us to isolate the weaker modulatory signals from the far surround, presumed to be mediated by feedback connections (Figs. 1a, b).

Contrast-dependence of surround suppression strength: experimental data

Near and far surround suppression: example responses

We measured patch-size tuning curves for 80 cells in macaque parafoveal V1 (2° – 8° eccentricities) by stimulating each cell with circular patches of drifting sinusoidal gratings of increasing radius at high and low contrast, and measuring the cell's response as a function of the patch radius (the “expanding patch method”). Our V1 sample

included cells from all layers, as determined from histological reconstruction of recorded cell location (the laminar data are reported in a previous study) ([Shushruth et al., 2009](#)). In addition, most cells in our sample had complex RFs (71 of 80 cells), therefore in the analysis we make no distinction between simple and complex RFs.

The left panels in Figs. 2a–c show patch-size tuning curves for three example cells, measured at high and low stimulus contrast. As previously reported, responses increased with increasing patch radius up to a peak, and then showed response suppression, and the patch radius at peak response (arrows) was larger at low than at high stimulus contrast ([Sceniak et al., 1999](#); [Sengpiel et al., 1997](#)). In our model this contrast-dependence of the patch radius at peak response occurs because at low contrast horizontal inputs must be summed over a larger area in order to bring the inhibitory neurons above firing threshold. The cells in Fig. 2, however, differed in the contrast-dependence of their asymptotic response. Whereas the mean firing rate at asymptotic response was the same at high and low contrast for the cell shown in the left panel of Fig. 2a, it was lower at low contrast than at high contrast for the cell in Fig. 2b (left panel). The majority of cells in our sample responded like the cells in Figs. 2a, b. However, for about a third of the population (27% of cells) the mean firing rate at the asymptotic response was higher at low than at high contrast; one such cell is shown on the left panel of Fig. 2c. Despite these differences, all three example cells in Fig. 2 (left panels) showed stronger surround suppression at high than at low contrast (values of suppression strength for each cell at each contrast level are reported in the legend to Fig. 2).

For 70 neurons, for which we measured patch-size tuning curves, we also obtained annulus-size tuning curves. To investigate the contrast dependence of far surround suppression, the expanding annulus method was performed at three different contrast conditions: high contrast center and surround (HH), low contrast center and high contrast surround (LH), and low contrast center and surround (LL). High and low contrast values were the same as used to measure patch-size tuning curves for the same neurons.

The right panels in Fig. 2 show annulus-size tuning curves for the same three cells shown in the left panels. In all three cells, the response in the HH condition (*black curve*) decreased as the inner radius of the annular grating was decreased, i.e. as more of the far surround region was stimulated (read the *x*-axes on the right panels of Fig. 2 from right to left). In our model this occurs because at high center contrast the inhibitory neurons are above firing threshold, and additional inputs to the RF center, via feedback and horizontal connections, further increase their responses (Fig. 1b). In the low contrast conditions (LH and LL, *red* and *gray curves*, respectively), responses were typically lower than in the HH condition, because the RF center was more weakly stimulated. Far surround suppression in the low contrast conditions was either weaker than in the HH condition (e.g. Figs. 2a, c right panels) or absent (e.g. Fig. 2b right panel). Although the model cannot account for such variability in the measured suppression, it predicts weaker suppression at low than at high center stimulus contrast (Fig. 1d).

Near and far surround suppression: population statistics

For each patch-size tuning curve at high and low contrast we measured the strength of surround suppression (SS_{patch}) as illustrated in the inset of Fig. 3a, and as detailed in [Materials and methods](#). $SS_{\text{patch}} = 0\%$ indicates complete lack of suppression, whereas $SS_{\text{patch}} = 100\%$ indicates that the cell's response was completely suppressed by the largest grating patch. Suppression strength varied significantly at both high (mean $65.8\% \pm 2.1$) and low (mean $49.5\% \pm 2.8$) contrast levels, and cells that were strongly and weakly suppressed were found at both high and low contrast. Notably, we found virtually no cells with $SS_{\text{patch}} < 20\%$ at high contrast (Figs. 3a, c). Importantly, surround suppression was significantly stronger at high than at low contrast (84% of cells are

above the unity line in Fig. 3a; $p < 10^{-6}$, paired Student's *t*-test). There was a significant correlation between suppression strength at high contrast and that at low contrast ($r = 0.58$, $p < 10^{-6}$; Pearson's correlation).

In contrast to these results, Sceniak et al. (1999), using a similar expanding patch protocol as in our study, reported that surround suppression is independent of stimulus contrast. In order to reconcile our results with those of Sceniak et al. (1999), we applied to our data these authors' measure of suppression strength, which involved fitting the patch-size tuning data with the DOG model, and measuring the ratio of the area under the inhibitory Gaussian over that of the excitatory Gaussian (see Materials and methods). In contrast, in the remainder of the paper we measured suppression strength with respect to response magnitude (i.e. as in the panel of Fig. 3a). Using the Sceniak et al. (1999) measure of suppression strength, we found that the contrast dependency of suppression strength was reversed, i.e., there was significantly stronger suppression at low contrast (Fig. 3b; $p = 0.0011$, two-sample *t*-test). Sceniak et al. (1999), indeed also reported slightly higher suppression at low contrast, but in their data set this trend was not statistically significant. These results indicate that the discrepancy between the contrast-dependent surround suppression we measured and the contrast-independent surround suppression reported by Sceniak et al. (1999) is in fact due to the different methods of quantifying

surround suppression (see Discussion). In the remainder of our study, however, we have used our method of quantification, because this involves only the measured responses and does not presuppose any particular statistical model.

Fig. 3d shows the distribution of the difference (Δ) in the strength of surround suppression between the low and high contrast conditions, estimated for each cell. Negative values indicate that suppression is weaker at low than at high contrast. About 84% (67 out of 80 cells) of cells in our sample had a negative value of ΔSS_{patch} (mean $-16.3\% \pm 2.3$), indicating weaker suppression at low stimulus contrast.

We then tested the model's prediction of weaker far surround suppression for lower contrast stimuli presented to the RF center. For each cell we measured the strength of far surround suppression from the annulus-size tuning data (SS_{annulus}) as illustrated in the inset of Fig. 4a (see Materials and methods). In the analysis reported in this paper, the suppression was measured with respect to the center-only response. However, we also performed the same analysis for suppression measured with respect to the maximum response over all annulus sizes (which would take into account facilitatory effects of surround stimulation); both analyses yielded similar results. The scatter plot in Fig. 4a shows, for each neuron, the strength of far surround suppression in the two low contrast conditions (LH and LL)

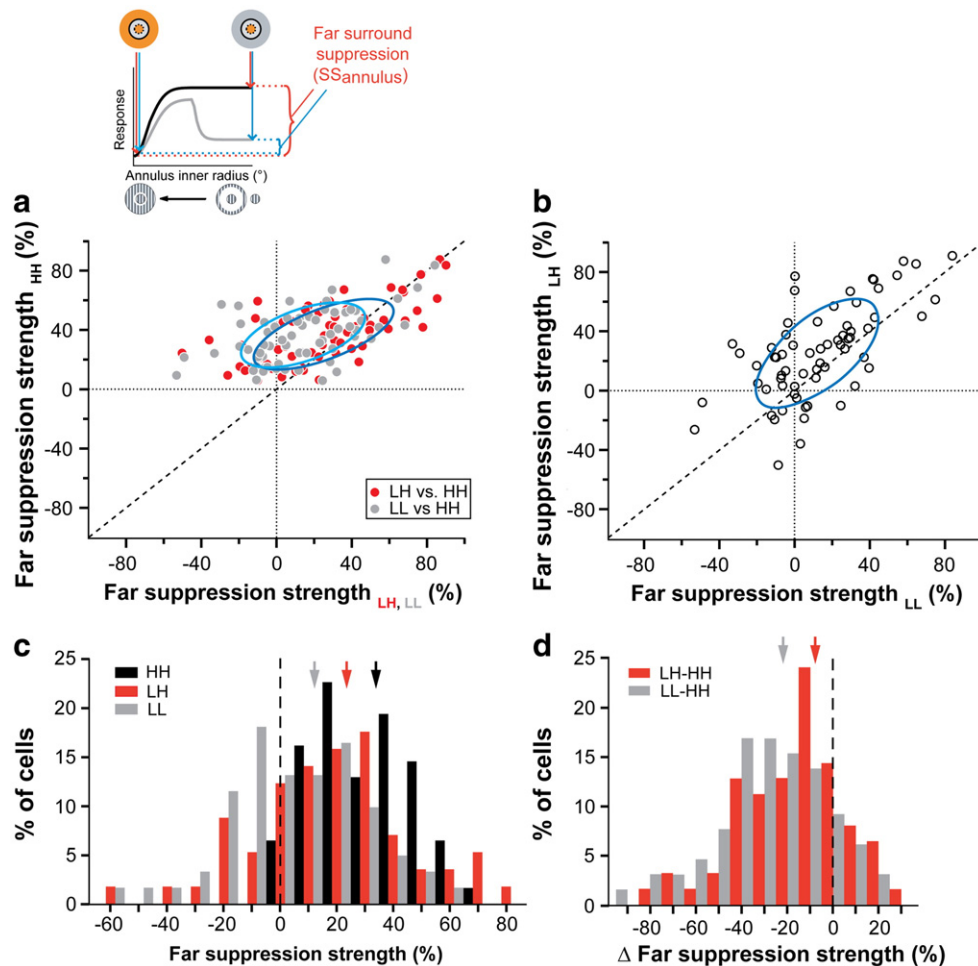


Fig. 4. Contrast-dependence of far surround suppression strength measured with expanding annulus protocol. (a) *Top inset:* Method used to compute the strength of far surround suppression from annulus-size tuning curves at high and low contrast (see also Materials and methods). *Bottom:* Scatter plot of far surround suppression strength in the high contrast condition (HH) vs. the two low contrast conditions (LH and LL, as indicated in legend). The blue ellipses indicate the 50% confidence intervals of the Gaussian fits to the data for the HH vs. LH (dark blue; $n = 63$ cells) and HH vs. LL (light blue; $n = 66$ cells) conditions. (b) Scatter plot of far surround suppression strength in the two low contrast conditions (LH vs. LL; $n = 64$ cells). (c) Distribution of far surround suppression strength in three different contrast conditions (according to legend), measured as indicated in (a). Arrows: medians (35.7%, 24.9% and 11.7% for HH, LH and LL, respectively). (d) Distribution of the change (Δ) in suppression strength with contrast, computed for each cell. Negative values of Δ indicate that suppression strength was stronger in the HH condition. Arrows: medians (-22.7% red; -7.5% gray).

compared to the high contrast (HH) condition. Most cells (70% of the *red dots*, and 82% of the *gray dots*) are above the unity line, indicating stronger suppression in the HH than in the LH or LL condition. Comparing far suppression strength in the two low contrast conditions, LH vs. LL (Fig. 4b) revealed that a lower contrast far surround stimulus exerts weaker suppression of the same low contrast center stimulus than a higher contrast far surround stimulus (72% of cells are above the unity line; $p < 0.02$). In summary, far surround suppression is weaker when the center stimulus is at lower contrast and it is even weaker when the surround is also at low contrast. The latter result is consistent with the mechanism operating in the model, because in the LH condition the higher contrast surround stimulus drives the center inhibitory neurons more strongly than the lower contrast surround stimulus in the LL condition. Figs. 4c, d shows two different quantifications of these results. Specifically, Fig. 4c shows the distribution of far suppression strength for the population in the three difference contrast conditions. Mean suppression strength in the two low contrast conditions (LH: $25.1\% \pm 3.9$, LL: $13.7\% \pm 3.4$) was significantly weaker than in the high contrast condition (HH: $37\% \pm 2.3$; $p < 0.001$ for HH vs. LH and $p < 10^{-6}$ for HH vs. LL in paired t -tests). Note also that in the low contrast conditions, but not in the high contrast condition, some cells (20% for LH, and 36% for LL) showed surround facilitation rather than suppression (see also Ichida et al., 2007). Fig. 4d shows, for each cell, the distribution of the difference in the strength of far surround suppression between the low and high contrast conditions ($\Delta SS_{\text{annulus}}$). Most cells showed negative values of $\Delta SS_{\text{annulus}}$, and the latter was significantly ($p < 10^{-10}$, paired t -test) lower for the LL-HH condition (mean $\Delta SS_{\text{annulus}} = -22.3\% \pm 2.9$) than for the LH-HH condition (mean $\Delta SS_{\text{annulus}} = -11.9\% \pm 3$).

We hypothesized that the near surround may exert stronger suppression than the far surround, because all three types of connections (feedforward, horizontal and feedback) contribute to the former, while only feedback contributes to the latter. To compare the strength of suppression from the near and far surround, in Fig. 5a we plot for each cell at high and low contrast the absolute suppression strength induced by the grating patch (SS_{patch}) vs. the strength of far surround suppression induced by the annular grating (SS_{annulus}). Virtually all cells in Fig. 5a are above the unity line (100% of *black dots*, 77% of *filled gray dots*, and 91% of *empty gray dots*), indicating that for almost all cells at both high and low contrast $SS_{\text{patch}} > SS_{\text{annulus}}$ ($p < 10^{-10}$, paired t -test for all contrast conditions). SS_{patch} and SS_{annulus} were also significantly correlated at both high contrast (high vs. HH: $r = 0.32$, $p = 0.007$, Pearson's correlation) and low contrast (low vs. LH: $r = 0.32$, $p = 0.0095$; low vs. LL: $r = 0.41$, $p = 5.6 \cdot 10^{-4}$), suggesting that the near and far surround may share similar suppressive mechanisms. In Supplementary Fig. 2 we demonstrate that the weaker suppression produced by far surround stimulation is not simply due to the smaller surround area stimulated with the annular grating, compared to that stimulated with the patch. When normalized by area, near surround suppression was much stronger than far surround suppression. These data are also consistent with previous studies showing that far surround modulation is weaker than near surround modulation (Ichida et al., 2007; Levitt and Lund, 2002; Shushruth et al., 2009).

We next compared quantitatively the magnitude of the contrast-dependence of suppression strength induced by near surround stimulation vs. far surround stimulation. We normalized suppression strength at low contrast to suppression strength at high contrast. In Fig. 5b, we plot for each cell this suppression strength ratio for near surround stimulation, measured from the patch-size tuning curve (SS_{patch} at low contrast/ SS_{patch} at high contrast), vs. the ratio for far surround stimulation, measured from the annulus-size tuning curve (SS_{annulus} at LH/ SS_{annulus} at HH, *black dots*; or SS_{annulus} at LL/ SS_{annulus} at HH, *gray dots*). A ratio = 1 indicates that the suppression at low contrast is the same as at high contrast, while a ratio < 1 indicates weaker suppression at low contrast. Although the suppression

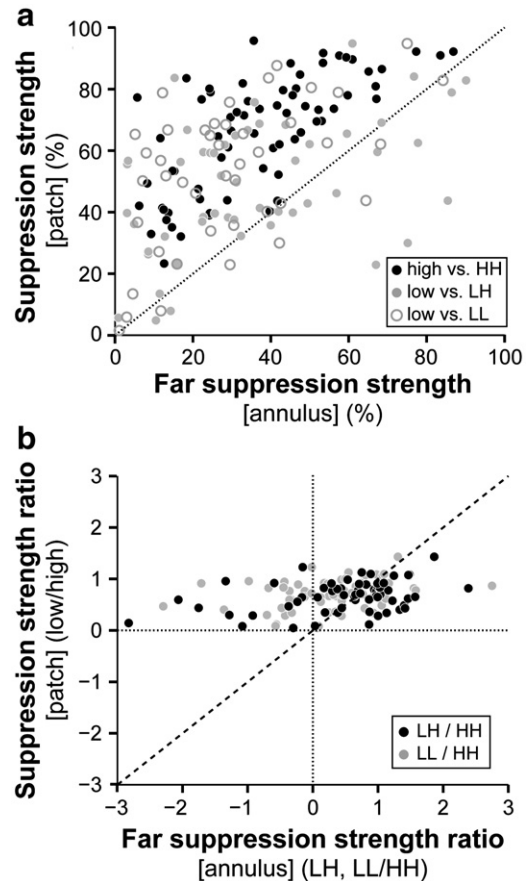


Fig. 5. Comparison of suppression strength measured with expanding patch (near) vs. suppression strength measured with expanding annulus (far). (a) Scatter plot of absolute strength of suppression measured with patch vs. measured with annulus at high and low contrast ($n = 69, 64, 67$ *black, filled gray and empty gray dots*, respectively). (b) Scatter plot of the ratio in suppression strength measured from patch-size tuning curves vs. the ratio in suppression strength measured from annulus-size tuning curves for each low contrast condition (LH and LL). Negative values of the ratio indicate surround facilitation. $n = 63$ and 66 *black and gray dots*, respectively.

strength ratio was < 1 for both near and far surround stimulation, it was significantly larger for near than for far surround stimulation. Specifically, for near surround stimulation, the suppression strength ratio averaged 0.68 ± 0.04 , while for far surround stimulation, it averaged 0.54 ± 0.13 (LH/HH) or 0.25 ± 0.15 (LL/HH). The mean difference of these ratios (SS_{patch} ratio - SS_{annulus} ratio) calculated for each cell was -0.14 ± 0.12 for the *black dots*, and -0.44 ± 0.14 for the *gray dots* in Fig. 5b; both means were significantly different from zero ($p < 10^{-10}$ for both; paired t -test). These results indicate that the magnitude of the contrast-dependent change in suppression strength is larger for far than for near surround suppression. This difference largely results from weaker suppression being induced at low contrast by far surround stimuli compared to near surround stimuli. Again this result emphasizes that while both near and far surround suppression likely share similar suppressive mechanisms, far surround suppression is weaker than near surround suppression, and this difference is even more pronounced at low contrast.

Contrast-dependence of surround suppression strength: data-model comparison

Surround suppression strength measured by the expanding patch method

In the original published version of our recurrent network model, we assumed, following available experimental data from rat visual cortex (Johnson and Burkhalter, 1996), that feedback connections do

not directly target inhibitory neurons, and that the latter are driven mainly by horizontal connections (Hirsch and Gilbert, 1991; McGuire et al., 1991). We demonstrated that despite this constraint, stimuli in the far surround could exert suppressive modulations on center responses via feedback connections targeting monosynaptic horizontal connections, which in turn target inhibitory neurons in the center (Fig. 1b). However, direct monosynaptic feedback excitation of inhibitory neurons is an alternative connection scheme that is strongly

suggested by more recent anatomical evidence from macaque monkey. In particular, Anderson and Martin (2009) have shown, albeit for a very small sample of V2 feedback axons, that the latter can form ~14% of their synapses in V1 with putative GABAergic targets.

Therefore, we have first characterized the consequences on the predicted strength of surround suppression, of changing the values of two key model parameters, i.e. the strength of horizontal and feedback excitation of inhibitory neurons. Figs. 6a, b shows how the

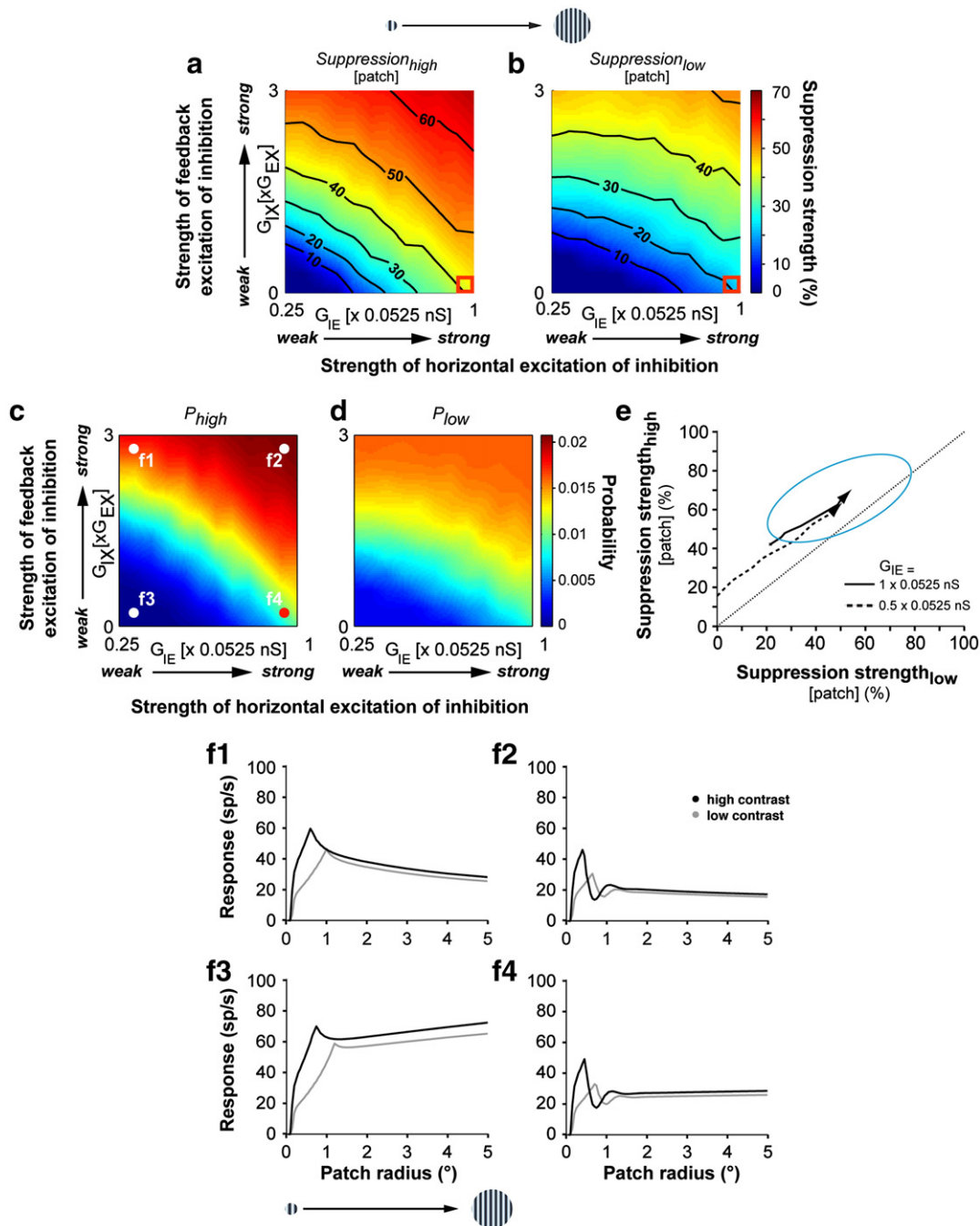


Fig. 6. Surround suppression strength measured with expanding patch: data-model comparison. (a, b) Plots of SS_{patch} at high (a) and low (b) contrast predicted by the model for different strengths of horizontal and feedback excitation of inhibition (G_{IE} and G_{IX} , respectively). Lines of iso-suppression strength are marked in (a–b), with numbers indicating suppression strength. (c, d) Comparison of the predicted and experimentally measured SS_{patch} . Plots of the probability of the predicted SS_{patch} , given the probabilistic description of the data (see Materials and methods) at high (c) and low (d) contrast. The model's predicted SS_{patch} is closer to the experimentally measured suppression for parameter regimes corresponding to strong lateral and feedback excitation of inhibition (upper right corner). (e) Predicted SS_{patch} at high and low contrast for increasing strengths of feedback excitation of inhibitory neurons (arrows point towards stronger feedback excitation of inhibition). The two different arrows indicate two different strengths of horizontal excitation of inhibition, namely the value used in the original model parameterization (solid line), and 50% of this value (dashed line). The blue ellipse corresponds to the ellipse in Fig. 3a. (f1–f4) Simulated patch-size tuning curves for the different parameter regimes marked as f1–f4 in panel (c). SS_{patch} in f1, f2, f3, f4 = 52%, 62%, 0% and 42% at high contrast, and 45%, 48%, 0% and 21% at low contrast, respectively.

simulated strength of surround suppression (measured from patch size tuning curves) depends on the values of these two model parameters. For both high (Fig. 6a) and low (Fig. 6b) contrast stimuli, the predicted suppression strength increases with stronger horizontal excitation of inhibitory neurons. Likewise, the predicted suppression strength increases with stronger feedback excitation of inhibitory neurons. For all combinations of values of these two model parameters, suppression was weaker for low contrast stimuli (Fig. 6b) than for high contrast stimuli (Fig. 6a). Thus, this key prediction, which we observed in the experimental data, is unchanged by variations in the values of these two model parameters. We then quantitatively compared the predicted suppression strength with the experimentally measured suppression strength, for these parameter combinations. The model in Schwabe et al. (2006) assumed strong horizontal excitation of local inhibitory cells, and no feedback excitation of inhibition, hence, it corresponds to the bottom right corner in the explored parameter space (red square in Figs. 6a, b). This parameter combination results in a model prediction of about 40% suppression strength at high contrast and about 20% at low contrast. Therefore, the model of Schwabe et al. (2006), in its original parameterization, cannot fully account quantitatively for the mean strength of suppression seen in our patch-size tuning data (65.8% at high contrast, and 49% at low contrast; see Figs. 3a, b). The suppression strength we measured experimentally, however, was variable; hence expressing it only in terms of mean suppression strength may disregard potentially important information for comparing the data with the model. The network model, on the other hand, is a model of mean responses, and it makes no prediction of the variability between cells in the data. Therefore, to exploit the variability measured in the data for a comparison with the model's predictions, we derived a probabilistic description of the suppression strengths in the data, in terms of a multivariate Gaussian probability distribution (see *Materials and methods*). The ellipse in Fig. 3a (like the ellipses in Figs. 4a, b) represents the 50% confidence interval for these fits. The ellipses are elongated and tilted, because they also capture the direction of scatter in the data. Then, we asked the following question: "How probable is the predicted strength of suppression, for high and low contrast stimuli, under this probabilistic description of our data?" In other words, how likely is it that we would have measured the predicted suppression strength? Note that while Schwabe et al.'s (2006) model sits at the bottom right corner of the explored parameter space (red point marked as f4 in Fig. 6c), different combinations of parameter values are as probable as the model in the original parameterization. The iso-probability lines in the plots of Figs. 6c, d are determined by the iso-suppression lines in Figs. 6a, b, because the latter indicate parameter regimes in which the model predicts the same strength of suppression. Hence, they are equally compatible with the data and are assigned the same probability. In Fig. 6e, the arrows indicate, for two different strengths of lateral excitation of inhibitory neurons (G_{IE}), the model's predicted suppression strengths at high and low contrast, as we increased the strength of monosynaptic feedback to inhibitory neurons (G_{IX}). Both parameter explorations end approximately in the center of the error ellipse (which is the same as in Fig. 3a), indicating that both predict suppression strengths which approximate the mean suppression strength in the data. However, while for all parameter regimes the suppression strength is lower at low than at high contrast (Fig. 6b vs. a), the best quantitative match with the measured suppression strength in the data was predicted for strong feedback excitation of inhibitory neurons. This is not the parameter regime that was used in the original published model, in which, there was no feedback excitation of inhibitory neurons (Schwabe et al., 2006).

Figs. 6f1–f4 shows model simulations of patch-size tuning curves under different parameter settings (corresponding to the dots in Fig. 6c). While strong horizontal excitation of inhibitory neurons leads to strong suppression, which asymptotes at small stimulus sizes ($<2^\circ$;

Figs. 6f2, f4), weak horizontal excitation of inhibitory neurons results in weaker suppression, which asymptotes at larger stimulus sizes (Fig. 6f1). In particular, weak horizontal excitation of inhibitory neurons reveals the spatially more extensive suppression arising from the far surround, mediated by feedback connections; this is because the surround stimulus continues to suppress the center response at distances from the RF center beyond the extent of horizontal connections. Obviously, if the inhibitory neurons are driven neither by horizontal nor feedback connections, the surround is predicted to facilitate the center response for any stimulus size and contrast (Fig. 6f3). Finally, compared to our original model parameterization (Fig. 6f4), strong lateral and feedback excitation of inhibitory neurons (Fig. 6f2) leads to stronger suppression at both high and low contrast, closer to the experimentally measured suppression strength. Note that the predicted responses in the high and low contrast conditions are similar, but the differences in the peak responses indicate weaker surround suppression at low contrast.

Surround suppression strength measured by the expanding annulus method

We then determined how the predicted strength of far surround suppression is affected by changes in the strength of horizontal and feedback excitation of inhibitory neurons. To this purpose we measured suppression strength on simulated annulus-size tuning curves under different parameter regimes. To ensure a fair comparison of the model predictions with the data, for the simulated experiments, the size of the center grating stimulus was adjusted to match the size of the sRF_{high} measured for each of the explored parameter configurations. This is because different combinations of the explored parameters affect the size of the sRF_{high} (see Figs. 6f1–f4). The predicted far surround suppression strengths at high (HH) and low (LH) center stimulus contrast are shown in Figs. 7a and b, respectively, for all model parameterizations (the predicted far surround suppression strength in the LL condition is shown in Supplementary Fig. 1). For all combinations of values of these two model parameters, suppression was weaker at low (LH or LL) compared to high center stimulus contrast (HH). Only for strong horizontal and feedback connections to inhibitory neurons (upper right corner in Figs. 7a, b) did the predicted suppression strengths in the HH and LH (and LL) conditions have similar maximal strength. In the HH and LH conditions the model in the original parameterization (red square in Figs. 7a–b) predicted suppression strengths of 56.7% and 33%, respectively (predicted suppression strength in the LL condition was 23.8%—see Supplementary Fig. 1). Therefore, the model of Schwabe et al. (2006), in its original parameterization, can account quantitatively for the experimentally measured far suppression strength; in fact, it predicts even stronger mean suppression than that seen in the annulus-size tuning data (37%, 25% and 14% in the HH, LH and LL conditions, respectively; see Fig. 4c). We then determined the probability of the predicted strength of suppression, given the probabilistic description of our data. As in Figs. 6c–d, the iso-suppression lines in Figs. 7a, b determine the iso-probability lines in the plots of Figs. 7c–d. Note that the original model parameterization, with strong horizontal excitation of inhibition and no feedback connections to inhibitory neurons (red point marked as f4 in Fig. 7c), predicts strong suppression. However, stronger feedback connections to inhibitory neurons also lead to far surround suppression strengths compatible with the measured suppression strengths in the data, over a wide range of values of horizontal connections' strengths. In Fig. 7e, the arrows indicate, for two different strengths of lateral excitation of inhibitory neurons (G_{IE}), the model's predicted suppression strengths in the HH and LH conditions, as we increased the strength of monosynaptic feedback to inhibitory neurons (G_{IX}). When the strength of the horizontal connections was set to 50% of the value used in the original model parameterization (dashed line), the model

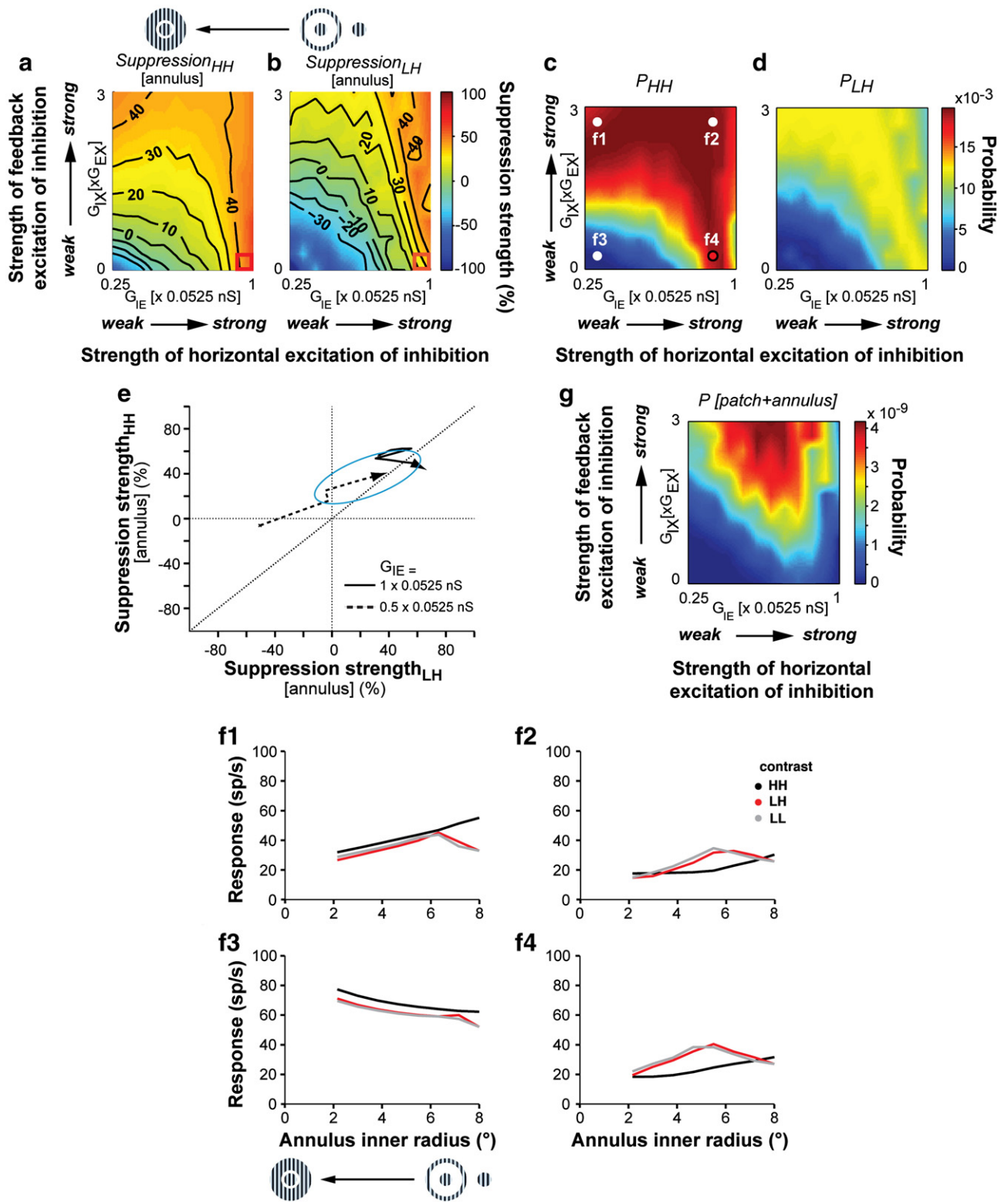


Fig. 7. Surround suppression strength measured with expanding annulus: data-model comparison. (a, b) Plots of $SS_{annulus}$ in the HH (a) and LH (b) contrast conditions predicted by the model for different strengths of horizontal and feedback excitation of inhibition (G_{IE} and G_{IX} , respectively). (c, d) Comparison of the predicted and experimentally measured $SS_{annulus}$. Plots of the probability of the predicted $SS_{annulus}$, given the probabilistic description of the data (see Materials and methods) in the HH (c) and LH (d) contrast conditions. (e) Predicted $SS_{annulus}$ in the HH and LH contrast conditions for increasing strengths of feedback excitation of inhibitory neurons (arrows point towards stronger feedback excitation of inhibition). The two different arrows indicate two different strengths of horizontal excitation of inhibition, namely the value used in the original model parameterization (solid line), and 50% of this value (dashed line). The blue ellipse corresponds to the ellipse in Fig. 4a. (f1–f4) Simulated annulus-size tuning curves for the different parameter regimes marked as f1–f4 in panel (c). $SS_{annulus}$ in f1, f2, f3, f4 = 42%, 42%, -24%, 42% (HH), 19%, 42%, -36%, 27% (LH) and 12%, 42%, -33%, 18% (LL), respectively. (g) Comparison of the model's predicted SS_{patch} and $SS_{annulus}$ considered together with those measured experimentally. Other conventions are as in Fig. 6.

predicted facilitation of the center response by the surround annulus for weaker values of feedback connections' strength, and suppression for stronger feedback connections. Instead for strong horizontal connections (solid line, as in the original model parameterization) all values of feedback connections' strength predicted suppression. Note that the origin of the solid line is close to the center of the ellipse. This indicates that the model in its original parameterization can predict the measured suppression strength in the annulus-size tuning data. However, the same mean values of far surround suppression strength can also be captured by a model parameterization corresponding to weaker horizontal and stronger feedback excitation of inhibitors than in the original model (end of the dashed line).

Figs. 7f1–f4 shows model simulations of annulus-size tuning curves in the HH, LH and LL conditions under different parameter settings (corresponding to the dots in Fig. 7c). Weak horizontal and feedback connections to inhibitory neurons generate facilitation at all contrast conditions (Fig. 7f3). Strong feedback and weak horizontal connections to inhibitors generate suppression at all annulus sizes in the HH condition, but in the LH and LL conditions they cause facilitation for smaller surround stimuli, and suppression for larger surround stimuli (Fig. 7f1). Note that the initial facilitation at low center stimulus contrast is present for all model parameterizations (Figs. 7f1–f4). This results from local inhibition being inactive when the center is weakly stimulated, and no additional drive from an annulus in the far surround is present. At high center contrast, instead, local inhibition is active and any additional drive leads to suppression, even for small annulus sizes (Figs. 7f1, f2, f4). As long as the local inhibition in the model is activated by an annulus in the far surround [either via monosynaptic feedback (Fig. 7f1), or via feedback relayed by horizontal connections (Fig. 7f4), or via both pathways (Fig. 7f2)], the simulated size tuning curves are similar to the experimentally measured tuning curves (right panels in Figs. 2a–c). Although far surround facilitation is not prominent in the responses of the example cells shown in Fig. 2, in a previous study we have shown that many V1 cells show far surround facilitation in the LH and LL conditions (Ichida et al., 2007). Thus, the model regimes marked by dots f1, f2, f4 in Fig. 7c are not only plausible candidates in terms of the strength of predicted far surround suppression, but also in terms of the shape of the annulus-size tuning curves.

We have so far considered the probability of the predicted suppression in the patch- and annulus-size experimental protocols separately. We now consider the probability of the predicted suppression for both experimental protocols together (Fig. 7g). While the model without feedback connections to inhibitory neurons can predict the experimentally measured suppression in the annulus-size tuning data, as long as horizontal connections to inhibitory neurons are strong (Fig. 7c, dot marked f4), this parameterization is not likely (Fig. 7g) when the predictions for the experimentally measured suppression in the patch-size tuning data are considered as well. This is because in this regime, the latter form of suppression is underestimated (origin of solid line in Fig. 6e). Only for stronger feedback connections to inhibitors do the predictions match the measured mean suppression strength in the patch-size tuning data (end of lines in Fig. 5e). As a consequence, weak feedback connections to inhibitory neurons are ruled out when patch and annular surround suppression are jointly used to constrain the model. Similarly, with very strong feedback and horizontal connections we predict even stronger far surround suppression than that measured in the data (end of solid line in Fig. 7e). Only weakening the strength of horizontal connections to inhibitory neurons leads to predicted far surround suppression matching that measured in the data (end of dashed line in Fig. 7e). As a consequence, very strong horizontal connections are ruled out as well, leaving model predictions with intermediate horizontal connection strengths and strong feedback connections as the most probable (Fig. 7g), given the measured data in both experimental protocols.

Combined effect of center stimulus size and contrast on the strength of surround suppression

In **Results** above, we have shown that our model predicts stronger near and far surround suppression at higher than at lower center stimulus contrast. Our data reported above confirm this model prediction. However, in contrast to our findings, **Levitt and Lund (1997)** reported that surround suppression is stronger for lower contrast center stimuli, a result that was later confirmed by **Cavanaugh et al. (2002b)**. We hypothesized that the discrepancy between our results and those from previous studies may be due to different definitions of size and low contrast used for the center stimulus. In particular, **Levitt and Lund's (1997)** experimental protocol consisted of a center grating fitted to the radius of the sRF_{high} , presented at two contrast levels, high and low; this was surrounded by an annular grating of 75% contrast and 8° outer diameter abutting the center grating. For the center grating, these authors chose as high contrast a value of 75%, and as low contrast a value that evoked a response near the middle of the cell's contrast-response function. In our study, we used a similar experimental protocol, but a blank annulus separated the surround and center gratings, and both our high and low contrast values were tailored to the recorded cell's contrast-response; importantly we chose as low contrast a value significantly lower than that used in **Levitt and Lund (1997)**, i.e. in most instances the lowest contrast that evoked a reliable response from the cell (see also **Materials and methods**). **Cavanaugh et al. (2002b)** used as high contrast a fixed value of 50%, and as low contrast values intermediate between those used by **Levitt and Lund (1997)** and those used in the present study.

Using our network model with the original parameterization (**Schwabe et al., 2006**), we simulated responses to a stimulus consisting of a high contrast (75%) surround annulus of 8° outer radius abutting a center grating whose size was varied slightly above and below the optimal (i.e. the sRF_{high} , which in the simulation measured 0.47°). The center grating was presented at high contrast (75%, HH condition) or at low contrast (LH condition); the low contrast values were varied (between 20% and 60% contrast in the simulation). Suppression strength was measured with respect to the center alone response at each respective contrast. We then computed the difference (Δ) in surround suppression strength between the LH and HH condition, as done for Fig. 4d. Fig. 8a shows a 2D plot of the difference in suppression strength as a function of the radius of the center grating, and of the contrast of the center grating in the LH condition. A negative value of Δ indicates stronger suppression in the HH than in the LH condition. It is clear from this plot that a slight overestimate of the sRF_{high} radius, combined with a higher center contrast in the LH condition, can produce positive values of Δ , i.e. stronger suppression for lower center stimulus contrast, as in **Levitt and Lund (1997)**. On the other hand, for lower center contrast levels, comparable to those used in our study in the LH condition, any center stimulus size around the optimal produces negative values of Δ , i.e. stronger suppression for higher center stimulus contrast, as in the present study. Fig. 8b further illustrates this concept, by showing the predicted suppression strength for a 75% contrast surround stimulus combined with a center stimulus of 75% (HH condition), 50% or 30% contrast (LH conditions), as a function of the size of the center stimulus. Suppression at 75% center contrast is stronger than at 30% contrast for all center stimulus sizes, however stronger suppression is predicted for 50% center contrast than for 75% center contrast for larger center stimulus sizes; this is because at these center stimulus sizes the high contrast response is already suppressed compared to the maximal response generated by an optimally sized stimulus (here: 0.47°).

We conclude that both our results and our network model are consistent with the results of **Levitt and Lund (1997)** and **Cavanaugh et al. (2002b)**.

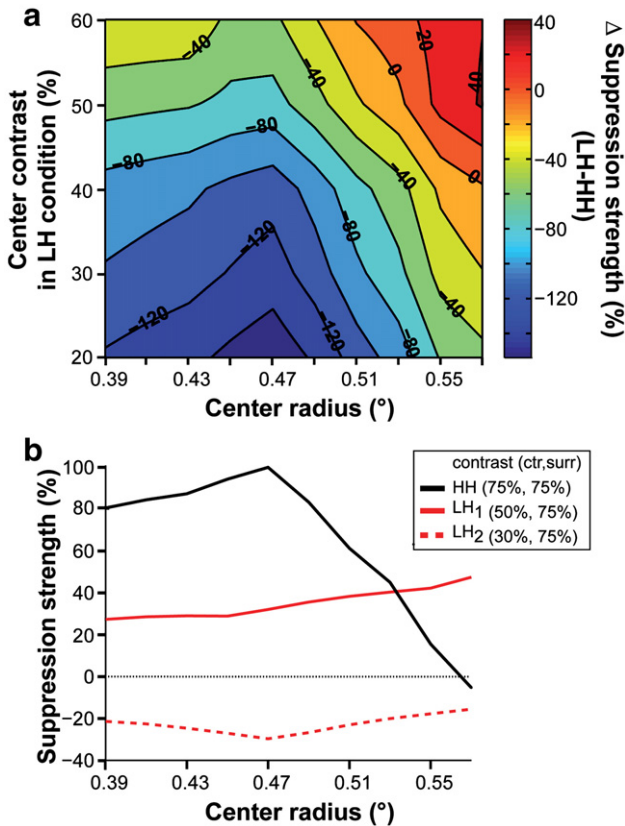


Fig. 8. Effect of center stimulus size and contrast on the predicted strength of surround suppression. (a) 2D plot of predicted Δ in surround suppression strength (SS in the LH condition–SS in the HH condition) as a function of the center grating patch radius, and of the low contrast level of the center grating patch in the LH condition. The cell's sRF_{high} radius in the simulation was 0.47° . The surround was an 8° annulus of fixed high contrast (75%) abutting the center grating, whose size was varied slightly above and below the sRF_{high} . The center contrast in the HH condition was 75%, while the contrast of the center grating in the LH condition was varied between 20% and 60%. (b) Predicted surround suppression strength at high (75%, HH) and low center contrast (50% or 30%, LH₁ and LH₂, respectively) as a function of the radius of the center grating patch (surround contrast was 75% for all three curves). Suppression strength in the HH condition is maximal at the optimal center stimulus size (i.e. when the center grating matches the radius of the recorded cell's sRF_{high}); for larger center stimulus radii, suppression progressively decreases (because the control “center-only” response is already suppressed at such center stimulus sizes), until it becomes weaker than suppression in the LH₁ condition. In the LH₂ condition, suppression is weaker than in the HH condition for any center stimulus radius.

Discussion

In this study, using single unit recordings in macaque V1, we have tested a prediction of a previously published recurrent network model (Schwabe et al., 2006) on the contrast dependence of surround suppression in V1. Specifically, the model predicted weaker near and far surround suppression when the RF center is stimulated with low contrast stimuli than when it is stimulated with high contrast stimuli. We have shown that our electrophysiological results are consistent with this model's prediction. Therefore surround suppression is weaker, and the spatial scale of signal integration is increased at low stimulus contrast.

Using a systematic parameter exploration, we have further quantitatively compared the strengths of the predicted and experimentally measured surround suppression. We found that the model in its original parameterization (which included strong horizontal, and no feedback excitation of local inhibitory neurons), can account quantitatively for the experimentally measured strength of far surround suppression, but cannot fully account for the strength of near surround suppression measured in the data. The parameter regime that best described quantitatively the experimentally mea-

sured near and far surround suppression included weaker horizontal and stronger feedback excitation of local inhibition than assumed in the original model.

Contrast-dependence of near surround suppression strength measured by the expanding patch method

It has previously been shown that stimulus contrast affects spatial summation in V1 (Kapadia et al., 1999; Sceniak et al., 1999; Sengpiel et al., 1997). While there is agreement that at low center stimulus contrast V1 RFs integrate signals over larger regions of visual space, the contrast-dependence of the suppressive effects of the surround has been less clear. Using the same expanding grating patch method used in the present study to measure suppression strength, some studies reported lower suppression strength for center and surround stimuli of lower contrast (Cavanaugh et al., 2002a; Sadakane et al., 2006). Instead, Sceniak et al. (1999) reported that suppression strength was independent of stimulus contrast. Here we have reproduced both findings, and demonstrated that the apparent discrepancy between them is due to different methods of quantifying suppression strength. While both measures of suppression strength are adequate, we have chosen to use the one that is based on measuring suppression with respect to response magnitude directly from the data, because this method does not presuppose any particular model. Importantly, our recurrent network model, albeit perhaps an oversimplification, does not affect the purely descriptive characterization of surround suppression in the data. In contrast, the measure used by Sceniak et al. (1999) assumes that surround suppression of center responses is realized by the summation over an excitatory center and a spatially more extensive inhibitory surround; but alternative mechanisms are also conceivable.

We conclude that the contrast dependence of near surround suppression strength observed in our experimental data is consistent with results from previous studies and with the prediction of our model.

Contrast-dependence of far surround suppression strength measured by the expanding annulus method

To test the model prediction on the contrast dependence of feedback-mediated far surround suppression, we used a center–annular surround stimulus designed to minimize afferent stimulation of feedforward and horizontal connection neurons in the near surround, and to isolate the weaker modulatory signals from the feedback-mediated far surround (Ichida et al., 2007). Consistent with the model's prediction, in our experimental measurements we found that a high contrast surround annulus induces weaker suppression of a low contrast center stimulus (LH condition) than of a high contrast center stimulus (HH condition); lowering the contrast of the surround stimulus in addition to that of the center stimulus (LL condition) decreases suppression strength even further. However, opposite to this finding, using a similar center–surround stimulus, previous studies reported that a high contrast surround stimulus suppresses a low contrast center stimulus more strongly than a high contrast one (Cavanaugh et al., 2002b; Levitt and Lund, 1997). Here, we have provided at least one possible interpretation for the apparent discrepancy between our results and results from these previous studies. In particular, we have shown that our model can generate opposite effects on the contrast-dependence of far surround suppression strength, depending on the size of the stimulus presented to the RF center, and the contrast level of the center stimulus chosen for the low contrast condition (when compared to the high contrast condition). According to this interpretation, choosing very low contrast levels for the center stimulus in the LH condition (as we have done) would produce weaker suppression at lower than at higher center contrast, irrespective of whether the sRF_{high} radius is

slightly over- or under-estimated. However, higher contrast levels of the center stimulus in the LH condition (e.g. as in [Levitt and Lund, 1997](#)) could produce the opposite result (i.e. stronger suppression at low center contrast), if the size of the cells' sRF_{high} is slightly overestimated. Therefore, our results on the contrast-dependence of far surround suppression strength are not inconsistent with those from previous studies, and our model is consistent with, and can account for, both findings.

Contrast-dependence of surround suppression in the network model

The model prediction of weaker near and far surround suppression for lower center stimulus contrast stems from the assumption that there exists a response asymmetry between excitation and inhibition ([Dragoi and Sur, 2000](#); [Schwabe et al., 2006](#); [Somers et al., 1998](#)), with suppression being mediated by local intracortical inhibition. For weak activation of the RF center (e.g. a low stimulus contrast) local inhibition is inactive. For strong activation (e.g. a high stimulus contrast in the RF center, or large surround stimuli activating horizontal and feedback connections), local inhibition crosses a threshold and suppresses the center response. Both the contrast-dependence of RF size and of surround suppression strength follow from this same assumption of response asymmetry between excitation and inhibition. The specific mechanism that we, and previously [Somers et al. \(1998\)](#), have proposed for its implementation (i.e. higher threshold and gain inhibitory neurons) is a specific and verifiable model's assumption, currently only partially supported by experimental data. For example, there have been reports in cortical layer 2/3 of high gain interneurons with facilitating synapses, whose response can only be recruited in the late phase of the action potential train of their presynaptic pyramidal cells ([Kapfer et al., 2005](#); [Pouille and Scanziani, 2004](#)). These facilitating interneurons could offer an alternative mechanism to higher threshold interneurons to implement the delayed recruitment of inhibition that is central to our model.

The response asymmetry between excitation and inhibition proposed in our model, could give rise to contrast-dependent spatial integration as described by the DOG model ([Sceniak et al., 1999](#)), or contrast-dependent divisive normalization as in the ratio-of-Gaussians model ([Cavanaugh et al., 2002a](#)); however, at the circuit-level it is realized by a network with fixed and contrast-independent connectivity. Other interpretations have employed the notion of functional connectivity. For example, recently [Nauhaus et al. \(2009\)](#) measured the interactions of neurons in V1 as a function of cortical distance and stimulus contrast. They concluded that the weight of horizontal connectivity dominates over that of feedforward connections at low contrast, and vice versa at high contrast. While this study provides strong evidence for stimulus-dependent coupling in V1, it is not conclusive with respect to the circuitry and mechanisms underlying it.

Thalamic surround suppression

Our model implements surround suppression in V1 using local intracortical inhibition and purely intracortical mechanisms, because it was specifically designed to investigate the cortical contribution to surround modulation. More specifically, our model was designed to account for responses in the superficial layers of V1, where both horizontal and feedback connections are prominent. While spatial summation and surround effects have generally been shown to occur in all V1 layers, subtle laminar differences do exist that may reflect laminar differences in anatomical connectivity. In particular, surround sizes are larger outside V1 input layer 4C ([Ichida et al., 2007](#)), which lacks horizontal and feedback connections, and surround suppression is stronger in the superficial than in the input layers ([Levitt and Lund, 2002](#); [Sceniak et al., 2001](#); [Shushruth et al., 2009](#)).

These laminar differences suggest that horizontal and feedback connections are needed to generate larger and stronger surrounds outside the input layer.

However, there is evidence that feedforward afferents from the lateral geniculate nucleus (LGN), which target neurons in layer 4C, contribute to V1 surrounds. First, LGN cells show extra-classical surround suppression ([Alitto and Usrey, 2008](#); [Bonin et al., 2005](#); [Sceniak et al., 2006](#); [Solomon et al., 2002](#)). Second, blockade of intracortical inhibition in cat V1 did not abolish V1 surround suppression measured by the expanding patch method ([Ozeki et al., 2004](#)). Third, two mechanisms have been shown to contribute to surround suppression in V1, one having broad spatio-temporal tuning (likely originating in the LGN), the other being sharply tuned for orientation, spatial and temporal frequency (likely generated intracortically) ([Webb et al., 2005](#)). However, there is also evidence that LGN surround suppression cannot fully account for V1 surrounds. First, while some have argued for orientation-tuned surround suppression in cat LGN ([Naito et al., 2007](#); [Sillito et al., 1993](#)), others have disagreed ([Bonin et al., 2005](#)); and evidence in primates indicates that LGN surrounds in this species are untuned for orientation ([Solomon et al., 2002](#); [Webb et al., 2002](#)). Therefore, at least in primates, intracortical mechanisms are needed to generate orientation-tuned surrounds. Second, the narrow spatial spread of macaque geniculocortical axons ([Angelucci and Sainsbury, 2006](#)), added to the small size of LGN surrounds ([Alitto and Usrey, 2008](#); [Sceniak et al., 2006](#)), cannot fully account for the large spatial scale of V1 surrounds ([Cavanaugh et al., 2002a](#); [Levitt and Lund, 2002](#); [Sceniak et al., 2001](#); [Shushruth et al., 2009](#)) (see [Fig. 1a](#)). Consistent with this notion is also our finding that V1 layer 4C lacks large surrounds ([Ichida et al., 2007](#); [Shushruth et al., 2009](#)), and that the largest surrounds in this layer are coextensive with the largest LGN surrounds. This suggests that layer 4C surrounds are inherited from the LGN, while the larger surrounds outside layer 4C are generated by intracortical connections. The most likely scenario is that V1 surround suppression inherits a spatially restricted orientation-untuned component of surround suppression from the LGN ([Webb et al., 2005](#); [Xing et al., 2005](#)), whose spatial scale is determined by that of geniculocortical afferents ([Angelucci and Sainsbury, 2006](#)). However, intracortical mechanisms based on intracortical inhibition, via horizontal and feedback connections, contribute a spatially broader and orientation-tuned component to V1 suppression ([Angelucci et al., 2002](#); [Cavanaugh et al., 2002b](#); [DeAngelis et al., 1994](#); [Ozeki et al., 2009](#); [Xing et al., 2005](#)).

Surround suppression in cat and primate LGN is also weaker at low than at high contrast ([Bonin et al., 2005](#); [Sceniak et al., 2006](#); [Solomon et al., 2002](#)). Therefore it is possible that the contrast-dependence of surround suppression strength in V1 may at least in part be inherited from the LGN.

Strength of surround suppression: data-model comparison

In its original version, the model was operated in a regime of strong horizontal and no feedback connections to local inhibitory neurons ([Schwabe et al., 2006](#)). This was motivated by the only anatomical data on the targets of feedback axons, available at the time we implemented the model. These data showed in rat that feedback neurons from extrastriate cortex target almost exclusively excitatory neurons in V1 ([Johnson and Burkhalter, 1996](#)), and exert predominantly excitatory influences on their target V1 cells ([Shao and Burkhalter, 1996](#)). We showed that despite this constraint, stimuli in the far surround could suppress center responses via feedback targeting monosynaptic horizontal connections to inhibitory neurons ([Schwabe et al., 2006](#)). Here we have demonstrated that when operated in a regime with no direct feedback contacts onto inhibitory neurons, the model can quantitatively account for the strength of far surround suppression, but cannot fully account for the strength of

near surround suppression. This suggests that additional inhibition is needed in the model to fully account for the suppression data. Recent anatomical data in macaque visual cortex have shown that V2 feedback axons can form about 14% of their synapses in V1 with putative inhibitory neurons (Anderson and Martin, 2009). Therefore, we have examined how adding direct feedback contacts onto inhibitory neurons could affect the strength of suppression. Specifically, we have performed a systematic quantitative comparison of the strength of suppression in the data with that measured in the model for different strengths of horizontal and feedback excitation of inhibitory neurons. We found that the parameter regime that can best describe both the near and far surround suppression data includes direct and strong feedback excitation of inhibitory neurons, coupled to weaker horizontal connections than in the original model. However, additionally or alternatively, the stronger inhibition needed in the model to account for the near surround data could arise from surround suppression of LGN afferents, which is missing in the current version of our model. We are currently testing this hypothesis.

Acknowledgments

Supported by: National Science Foundation Grant IOS-0848106 to A.A., National Eye Institute Grants EY015262 and EY019743 to A.A., and EY015609 to J.M.I., DFG Grant 803371 to L.S., Wellcome Trust Grant 061113, and a Research to Prevent Blindness Grant to the Department of Ophthalmology, University of Utah.

Appendix A. Supplementary data

Supplementary data associated with this article can be found, in the online version, at doi:10.1016/j.neuroimage.2010.01.032.

References

- Allitto, H.J., Usrey, W.M., 2008. Origin and dynamics of extraclassical suppression in the lateral geniculate nucleus of the macaque monkey. *Neuron* 57, 135–146.
- Allman, J., Miezin, F., Mc Guinness, E., 1985. Stimulus specific responses from beyond the classical receptive field: neurophysiological mechanisms for local-global comparisons in visual neurons. *Ann. Rev. Neurosci.* 8, 407–430.
- Anderson, J.C., Martin, K.A.C., 2009. The synaptic connections between cortical areas V1 and V2 in macaque monkey. *J. Neurosci.* 29, 11283–11293.
- Angelucci, A., Bressloff, P.C., 2006. The contribution of feedforward, lateral and feedback connections to the classical receptive field center and extra-classical receptive field surround of primate V1 neurons. *Prog. Brain Res.* 154, 93–121.
- Angelucci, A., Sainsbury, K., 2006. Contribution of feedforward thalamic afferents and corticogeniculate feedback to the spatial summation area of macaque V1 and LGN. *J. Comp. Neurol.* 498, 330–351.
- Angelucci, A., Levitt, J.B., Walton, E.J., Hupe, J.M., Bullier, J., Lund, J.S., 2002. Circuits for local and global signal integration in primary visual cortex. *J. Neurosci.* 22, 8633–8646.
- Blakemore, C., Tobin, E.A., 1972. Lateral inhibition between orientation detectors in the cat's visual cortex. *Exp. Brain Res.* 15, 439–440.
- Bonin, V., Mante, V., Carandini, M., 2005. The suppressive field of neurons in lateral geniculate nucleus. *J. Neurosci.* 25, 10844–10856.
- Cavanaugh, J.R., Bair, W., Movshon, J.A., 2002a. Nature and interaction of signals from the receptive field center and surround in macaque V1 neurons. *J. Neurophysiol.* 88, 2530–2546.
- Cavanaugh, J.R., Bair, W., Movshon, J.A., 2002b. Selectivity and spatial distribution of signals from the receptive field surround in macaque V1 neurons. *J. Neurophysiol.* 88, 2547–2556.
- DeAngelis, G.C., Freeman, R.D., Ohzawa, I., 1994. Length and width tuning of neurons in the cat's primary visual cortex. *J. Neurophysiol.* 71, 347–374.
- Dragoi, V., Sur, M., 2000. Dynamic properties of recurrent inhibition in primary visual cortex: contrast and orientation dependence of contextual effects. *J. Neurophysiol.* 83, 1019–1030.
- Friston, K.J., 2005. A theory of cortical responses. *Philos. Trans. R. Soc. Lond. B. Biol. Sci.* 360, 815–836.
- Gilbert, C.D., Wiesel, T.N., 1990. The influence of contextual stimuli on the orientation selectivity of cells in primary visual cortex of the cat. *Vision Res.* 30, 1689–1701.
- Girard, P., Hupe, J.M., Bullier, J., 2001. Feedforward and feedback connections between areas V1 and V2 of the monkey have similar rapid conduction velocities. *J. Neurophysiol.* 85, 1328–1331.
- Harrison, L.M., Stephan, K.E., Rees, G., Friston, K.J., 2007. Extra-classical receptive field effects measured in striate cortex with fMRI. *Neuroimage* 34, 1199–1208.
- Hirsch, J.A., Gilbert, C.D., 1991. Synaptic physiology of horizontal connections in the cat's visual cortex. *J. Neurosci.* 11, 1800–1809.
- Ichida, J.M., Schwabe, L., Bressloff, P.C., Angelucci, A., 2007. Response facilitation from the "suppressive" receptive field surround of macaque V1 neurons. *J. Neurophysiol.* 98, 2168–2181.
- Johnson, R.R., Burkhalter, A., 1996. Microcircuitry of forward and feedback connections within rat visual cortex. *J. Comp. Neurol.* 368, 383–398.
- Kapadia, M.K., Westheimer, G., Gilbert, C.D., 1999. Dynamics of spatial summation in primary visual cortex of alert monkeys. *Proc. Natl. Acad. Sci. U. S. A.* 96, 12073–12078.
- Kapfer, C., Pouille, F., Scanziani, M., 2005. Recurrent inhibition in layer 2/3 of the somatosensory cortex. *Soc. Neurosci. Abstr. Online. Program. No.* 968, 7.
- Knierim, J.J., van Essen, D.C., 1992. Neuronal responses to static texture patterns in area V1 of the alert macaque monkey. *J. Neurophysiol.* 67, 961–980.
- Lamme, V.A., 1995. The neurophysiology of figure-ground segregation in primary visual cortex. *J. Neurosci.* 15, 1605–1615.
- Levitt, J.B., Lund, J.S., 1997. Contrast dependence of contextual effects in primate visual cortex. *Nature* 387, 73–76.
- Levitt, J.B., Lund, J.S., 2002. The spatial extent over which neurons in macaque striate cortex pool visual signals. *Vis. Neurosci.* 19, 439–452.
- Li, Z., 1999. Visual segmentation by contextual influences via intra-cortical interactions in the primary visual cortex. *Network* 10, 187–212.
- Li, W., Piëch, V., Gilbert, C.D., 2008. Learning to link visual contours. *Neuron* 57, 442–451.
- Malik, J., Perona, P., 1990. Preattentive texture discrimination with early vision mechanisms. *J. Opt. Soc. Am. A* 7, 923–932.
- Maunsell, J.H., Treue, S., 2006. Feature-based attention in visual cortex. *Trends Neurosci.* 29, 317–322.
- McGuire, B.A., Gilbert, C.D., Rivlin, P.K., Wiesel, T.N., 1991. Targets of horizontal connections in macaque primary visual cortex. *J. Comp. Neurol.* 305, 370–392.
- Naito, T., Sadakane, O., Okamoto, M., Sato, H., 2007. Orientation tuning of surround suppression in lateral geniculate nucleus and primary visual cortex of cat. *Neurosci* 149, 962–975.
- Nauhaus, I., Busse, L., Carandini, M., Ringach, D.L., 2009. Stimulus contrast modulates functional connectivity in visual cortex. *Nat. Neurosci.* 12, 70–76.
- Navalpakkam, V., Itti, L., 2007. Search goal tunes visual features optimally. *Neuron* 53, 605–617.
- Nelson, J.L., Frost, B., 1978. Orientation selective inhibition from beyond the classical receptive field. *Brain Res.* 139, 359–365.
- Ozeki, H., Sadakane, O., Akasaki, T., Naito, T., Shimegi, S., Sato, H., 2004. Relationship between excitation and inhibition underlying size tuning and contextual response modulation in the cat primary visual cortex. *J. Neurosci.* 24, 1428–1438.
- Ozeki, H., Finn, L.M., Schaffer, E.S., Miller, K.D., Ferster, D., 2009. Inhibitory stabilization of the cortical network underlies visual surround suppression. *Neuron* 62, 578–592.
- Petrov, Y., McKee, S.P., 2006. The effect of spatial configuration on surround suppression of contrast sensitivity. *J. Vis.* 6, 224–238.
- Polat, U., Mizobe, K., Pettet, M.W., Kasamatsu, T., Norcia, A.M., 1998. Collinear stimuli regulate visual responses depending on cell's contrast threshold. *Nature* 391, 580–584.
- Pouille, F., Scanziani, M., 2004. Routing of spike series by dynamic circuits in the hippocampus. *Nature* 429, 717–723.
- Rao, R.P., Ballard, D.H., 1999. Predictive coding in the visual cortex: a functional interpretation of some extra-classical receptive-field effects. *Nat. Neurosci.* 2, 79–87.
- Sadakane, O., Ozeki, H., Naito, T., Akasaki, T., Kasamatsu, T., Sato, H., 2006. Contrast-dependent, contextual response modulation in primary visual cortex and lateral geniculate nucleus of the cat. *Eur. J. Neurosci.* 23, 1633–1642.
- Salinas, E., 2006. How behavioral constraints may determine optimal sensory representations. *PLoS Biol.* e387, 4.
- Sceniak, M.P., Ringach, D.L., Hawken, M.J., Shapley, R., 1999. Contrast's effect on spatial summation by macaque V1 neurons. *Nat. Neurosci.* 2, 733–739.
- Sceniak, M.P., Hawken, M.J., Shapley, R.M., 2001. Visual spatial characterization of macaque V1 neurons. *J. Neurophysiol.* 85, 1873–1887.
- Sceniak, M.P., Chatterjee, S., Callaway, E.M., 2006. Visual spatial summation in macaque geniculocortical afferents. *J. Neurophysiol.* 96, 3474–3484.
- Schäfer, R., Vasilaki, E., Senn, W., 2007. Perceptual learning via modification of cortical top-down signals. *PLoS Comput. Biol.* e165, 3.
- Schwabe, L., Obermayer, K., 2005. Learning top-down gain control of feature selectivity in a recurrent network model of a visual cortical area. *Vision Res.* 45, 3202–3209.
- Schwabe, L., Obermayer, K., Angelucci, A., Bressloff, P.C., 2006. The role of feedback in shaping the extra-classical receptive field of cortical neurons: a recurrent network model. *J. Neurosci.* 26, 9117–9129.
- Schwartz, O., Simoncelli, E.P., 2001. Natural signal statistics and sensory gain control. *Nat. Neurosci.* 4, 819–825.
- Sengpiel, F., Sen, A., Blakemore, C., 1997. Characteristics of surround inhibition in cat area 17. *Exp. Brain Res.* 116, 216–228.
- Shao, Z., Burkhalter, A., 1996. Different balance of excitation and inhibition in forward and feedback circuits of rat visual cortex. *J. Neurosci.* 16, 7353–7365.
- Shushruth, S., Ichida, J.M., Levitt, J.B., Angelucci, A., 2009. Comparison of spatial summation properties of neurons in macaque V1 and V2. *J. Neurophysiol.* 102, 2069–2083.
- Sillito, A.M., Cudeiro, J., Murphy, P.C., 1993. Orientation sensitive elements in the corticofugal influence on centre-surround interactions in the dorsal lateral geniculate nucleus. *Exp. Brain Res.* 93, 6–16.

- Solomon, S.G., White, A.J., Martin, P.R., 2002. Extraclassical receptive field properties of parvocellular, magnocellular, and koniocellular cells in the primate lateral geniculate nucleus. *J. Neurosci.* 22, 338–349.
- Somers, D., Todorov, E.V., Siapas, A.G., Toth, L., Kim, D.S., Sur, M., 1998. A local circuit approach to understanding integration of long-range inputs in primary visual cortex. *Cereb. Cortex* 8, 204–217.
- Webb, B.S., Tinsley, C.J., Barraclough, N.E., Easton, A., Parker, A., Derrington, A.M., 2002. Feedback from V1 and inhibition from beyond the classical receptive field modulates the responses of neurons in the primate lateral geniculate nucleus. *Vis. Neurosci.* 19, 583–592.
- Webb, B.S., Dhruv, N.T., Solomon, S.G., Tailby, C., Lennie, P., 2005. Early and late mechanisms of surround suppression in striate cortex of macaque. *J. Neurosci.* 25, 11666–11675.
- Xing, D., Shapley, R.M., Hawken, M.J., Ringach, D.L., 2005. Effect of stimulus size on the dynamics of orientation selectivity in Macaque V1. *J. Neurophysiol.* 94, 799–812.